The sequestration of trace metals preserved in pyritized burrows

Connor Brolly*[1], John Parnell[1] & Xueying Wang[2]

[1]University of Aberdeen, Department of Geology & Geophysics, Aberdeen AB24 3UE

[2]University of Aberdeen, Department of Chemistry, Aberdeen AB24 3UE

*Corresponding author: Connor Brolly, University of Aberdeen, AB24 3UE, connor.brolly@gmail.com

Abstract

Pyritized burrows from three localities were analysed using LA-ICP-MS to determine their trace element content and assess their ability to sequester trace elements. Pyritic burrows from Hock Cliff (Jurassic), Wren's Nest (Silurian) and Southerham Grey Pit (Cretaceous) have anomalous levels of Se, Cu and Pb and are enriched relative to their host sediments. Sequestration rates were calculated using sedimentation rates from similar depositional environments. Results show that pyritic burrows, mediated by bacterial sulphate reduction, can sequester Se, Cu and Pb up to 3 orders of magnitude greater than the rate of Fe-Mn crusts, which are considered rich sources of trace elements, demonstrating that bioturbated marine sediments are significant sinks of trace elements.

Keywords: Bioturbation, burrows, pyrite, trace elements, sequestration, selenium

1 Introduction

Burrows are one of a large range of trace fossils, which can be defined as a biogenic sedimentary structure created in sediment by the activity of a burrowing animal (Bromley, 1996). The burrows analysed in this study are cylindrical or tube-line sedimentary features which are present in all orientations (vertical to horizontal) in shallow marine environments and which are generally oxidised.

Burrowing evolved particularly at the Ediacaran-Cambrian boundary during a major increase in animal diversification and modes of life (Buatois et al., 2020; Mángano and Buatois, 2014). Burrowing in the Ediacaran was restricted to very small horizontal traces, commonly associated with firm, erosion-resistant algal mats (Jensen et al., 2006; Seilacher et al., 1999). The Cambrian Period is characterised by an increase in penetrative, vertical burrowing promoting the exchange of fluids and OM between the water column and the sediment, increasing habitability, known as the 'agronomic revolution' (Seilacher et al., 1999).

Sulphate-reducing bacteria control the composition of OM in shallow marine sediments under anoxic conditions, and higher microbial activity is coupled with decreasing sulphate levels and an increase of sulphide and OM degradation (Sturdivant and Shimizu, 2017). Burrows are commonly enriched in organic matter and a range of nutrients including nitrogen, potassium, phosphorus, sulphur, and trace elements as burrowing organisms such as worms, secrete mucus to pass easily through the sediment (Ayoola and Olayiwola, 2014; Bromley, 1996). The mucus in the burrow walls can be used as a feedstock for sulphate-reducing bacteria which promotes localised hydrogen sulphide (H_2S), and early diagenetic pyrite (Virtasalo and Kotilainen, 2013; Virtasalo et al., 2010). Pyritization would most likely take place after the death of the organism, as a live organism would create an oxic environment which would prohibit pyritization (Jørgensen, 1977). The decomposition of the mucus walls and the burrowing organism creates a reducing environment which favours pyrite formation (Thomsen and Vorren, 1984).

The reworking of sediments by animal activity prior to compaction alters the substrate significantly. Burrowing organisms such as worms can have subsurface burrows as deep as 2 m and affect several square kilometres of sediment (Gingras et al., 2015; Weaver and Schultheiss, 1983). Burrowing can highlight erosional features in fine grained sediments such as black shales, which reveals information on bottom currents, water-column mixing and oxygenation (Schieber, 2003). It can disturb sediment layering which enables the exchange of minerals and fluids between sedimentary layers; cause an

47 increase or decrease in organic matter and change the pore fluid chemistry. These changes have
48 knock-on effects on porosity and permeability, which is why bioturbation is an important area of
49 research for the oil industry, as it can affect oil recovery (Gingras et al., 2015; Pemberton and Gingras,
50 2005).

51 Bioturbation also has implications for trace element sequestration and concentration. Pyrite is a
52 major residence of trace elements in sedimentary rocks. It is more common for pyrite to precipitate
53 in sediments such as black shales that are clearly anoxic (Hu and Gao, 2008; Large et al., 2015, 2014;
54 Parnell et al., 2016). However, pyrite also precipitates in anoxic/sub-oxic microenvironments within
55 otherwise oxic environments (Jørgensen, 1977; Mitchell, 1968; Thomsen and Vorren, 1984), such as
56 the burrows investigated here. Pyritic burrows from three localities in the UK, representing a range of
57 geological ages were analysed to investigate their trace metal element and sequestration rate.

58 The objectives were to determine:

59 (i) If the burrow pyrite contains anomalous concentrations of trace elements. Pyrite in black
60 shale can concentrate trace elements first located in organic matter in the carbonaceous
61 sediment, but this reservoir is not available in many other sediments so enrichment in
62 pyrite might not occur.
63 (ii) If trace elements in the burrow pyrite represent concentrations relative to the host
64 sediment.
65 (iii) If the pyrite caused an overall sequestration of trace elements into the host bed.

66 ## 2 Methods

67 Pyritized burrows were collected from three localities throughout the UK (Fig. 1); Wren's Nest, Dudley
68 (Silurian), Hock Cliff, Fretherne (Jurassic) and Southerham Grey Pit, Lewes (Cretaceous). Wren's Nest,
69 Dudley, part of the Much Wenlock Limestone Formation, hosts extremely well preserved Silurian fossil
70 biota including pyritized burrows, which are concentrated in the Nodular Beds Member (Ray and

Thomas, 2007). The Blue Lias Formation, exposed at Hock Cliff, Fretherne, has alternating mudstones, shales and limestones, with vertical pyritized burrows preserved in dark, grey shale beds (Simms et al., 2004). Southerham Grey Pit, Lewes, has abundant 'worm' tubes, which are pyritized or have pyritized nodules spatially associated with them, found in the Zig Zag Chalk Formation (Jeans et al., 2016).

Mm-scale burrows from each locality were analysed by laser ablation-inductively coupled plasma-mass spectrometry (LA-ICP-MS) to produce enrichment maps. The LA-ICP-MS method is described in detail in Parnell et al. (2017). This approach was used to map the distribution of Fe, Se, Cu and Pb. These elements were chosen because they are commonly found in pyrite in black shales.

Average trace element values from Fe-Mn rich crusts and Neoproterozoic Gwna Group shales were used as a comparison with the new data presented here, given that both are regarded as rich sources of trace elements and the Gwna Group shales were studied at the same laboratory at the University of Aberdeen.

Bulk trace metal content was determined by inductively coupled plasma-atomic emission spectrometry (ICP-AES) and inductively coupled plasma-mass spectrometry (ICP-MS), at ALS Laboratories, Loughrea, Ireland. Each sample was agate milled and homogenised and 0.5 g was partially digested using aqua regia.

Scanning electron microscopy was performed on a Zeiss Gemini-300 FEG-SEM, to investigate mineralisation within the burrows.

3 Results

3.1 LA-ICP-MS

Burrows were analysed with LA-ICP-MS to determine the enrichment and the distribution of elements within an area of interest e.g. cross-section of a burrow. The trace metal content of the samples and

average shale and carbonate values are summarised in Table 1, and are plotted in Fig. 2. Average spot analyses from Hock Cliff burrows show a Se content of 8.2 & 7.7 ppm (A & B respectively). Mean shale Se content is 1.3 ppm (Stüeken et al., 2015). The average Pb content at Hock Cliff is 669 ppm in burrow A & 297 ppm in burrow B, which is up to 30 times higher than the global mean shale Pb content of 19.5 ppm (Hu and Gao, 2008). The average Cu content is 494 ppm in burrow A & 215 ppm in burrow B, which is up to 10 times higher than the global mean shale Cu content of 36.5 ppm (Hu and Gao, 2008). The host rock has a Se value of 0.7 ppm, a Cu value of 10.7 ppm, and a Pb value of 6.24 ppm.

Fe, Se, Cu and Pb LA-ICP-MS maps from Hock Cliff are shown in Fig. 3 below. Se and Pb are concentrated in the rim of both burrows suggesting they occur in the same mineral phase. In burrow A, Fe is more concentrated in the rim, suggesting there is some weathering in the burrow core. Cu is more evenly distributed but appears slightly depleted in the burrow rim.

Fe, Cu and Pb maps from Wren's Nest are shown in Fig. 4, below. The concentrations of Cu and Pb are more evenly distributed throughout the burrow, compared with Hock cliff where the Se and Pb are concentrated in a halo towards the edge of the burrow. Another notable feature is the lack of Se present within the burrow. Cu and Pb are concentrated in similar amounts compared with Hock Cliff.

Average spot analyses show a Cu content of 210 ppm, which is 5 times that of the global mean shale Cu content, and a Pb content of 198, which is 10 times that of the global mean shale Pb content (Hu and Gao, 2008). The Wren's nest host rock has a Cu content of 4 ppm, and a Pb content of 4.19 ppm.

Southerham burrows are extremely weathered and the majority of them display a weathered burrow core, which could not be analysed by LA-ICP-MS as the surface was not flat. The burrows are large enough to be extracted for bulk analysis at ALS laboratories which is comparable to LA-ICP-MS. The results are summarised in Table 1.

Pyritized burrow from Southerham have a Se value of 4.5 ppm, Cu of 66 ppm, and Pb of 329 ppm. These measured values are up to 15 times greater than the average shale values, and up to 2 orders of magnitude greater than the host rock values (Hu and Gao, 2008).

4 Discussion

4.1 Metal enrichment in burrows

A summary of the burrow forming process and metal enrichment is shown in Fig. 5 below. Trace metals are incorporated in to burrows during diagenesis. Trace metal-rich seas deposit a range of elements including Se, Pb and Cu on the seafloor. Iron-oxides present in the seafloor sediments act as a sink, and many trace elements are adsorbed on the Fe-oxides. Organic matter accumulates on the seafloor through the decomposition of marine organisms and land-derived detritus (e.g. plant material). Burrowing organisms introduce organic matter, Fe (oxyhydr)oxides and trace metal oxyanions into the burrow from the seafloor (Berner, 1984; Virtasalo and Kotilainen, 2013). The act of burrowing requires a lubricant; therefore, organisms secrete mucus to ease passage through the sediment which decays creating a localised reducing environment (Bromley, 1996). Lalonde et al. (2010) demonstrated that mucus linings were more reactive than other organic compounds in marine sediment, increasing the potential of burrows as metal sinks. Mucus trails preserved by pyritization are found in the Cretaceous Ingersoll shale where body fossils are not as common, emphasising the reactivity of mucus secreted by organisms (Savrda et al., 2016). Burrows preserve a range of nutrients such as nitrogen, potassium, phosphorus, sulphur, and trace elements as a result of the burrowing organism (Ayoola and Olayiwola, 2014).

The introduction of “super-reactive” organic carbon in the form of extracellular polysaccharides (EPS) bioturbation within the burrow system, through mucus lining of the burrower drives sulphate reduction and OM degradation (Harazim et al., 2020; Sturdivant and Shimizu, 2017; Sutherland, 2006). Early localised sulphate-reducing bacteria exploit OM in the burrow as a feedstock, reducing sea water

sulphate to hydrogen sulphide (H_2S). The H_2S reacts with iron minerals which are rich in trace metals to form pyrite. This process is dependent on a balance between carbon, sulphur, and iron. Bioturbation in iron-rich sediments rapidly oxidises OM through iron-reducing bacteria. Where no bioturbation occurs, sediments become sulphide rich, mediated by sulphate reducing bacteria. In Fe-rich sediments, the supply of ferrous iron exceeds the supply of sulphide and ferrous iron reacts with H_2S and sequesters it to monosulfide, which detoxifies the sediment, promoting bioturbation (Antler et al., 2019). At depth sediments become dominated by sulphide which is poisonous to bioturbating organisms and reduced ventilation from sediment mixing, inhibits the reoxidation of ferrous Fe, promoting pyrite formation (Antler et al., 2019). The trace metals present in the pyrite reflect the trace metals present in the iron minerals in the sediment (Mitchell, 1968). After diagenesis the burrow is completely pyritized and enriched in trace metals. Au, Cd, Cu, Pb and Zn are commonly found adsorbed onto naturally occurring Fe sulphides, and this process could be significant in the concentration of metals and the formation of ore deposits (Huerta-diaz et al., 1998; Jean and Bancroft, 1986).

The control that bioturbation has for mobility of redox-sensitive trace elements (i.e. Fe, V, Cr, Mn, Co, Ni, Cu, and As) has been addressed by Harazim et al., (2015). The authors found that the average TOC was 1.0 wt. % higher in sediment from within burrows compared with the surrounding sediment, and that pyrite found within burrows correlated with an increased level of Co, Ni, Cu and Zn. The rarity of the pyrite and persistence of organic carbon suggest that in this case the carbon was too refractory to be used as a feedstock for bacterial sulphate reduction (Widerlund and Davison, 2007). The lack of organic matter reactivity means that these elements are incorporated into silicates rather than pyrite or organic matter. The localities selected for this study were abundant in pyritized burrows suggesting that the bioavailability of the organic matter in the burrows was not a limiting factor.

Examples of lacustrine pyritic burrows are also found in the literature. Virtasalo et al. (2010), analysed small burrow-like and irregularly shaped concretions in Holocene postglacial lacustrine clays in the

northern Baltic Sea. The burrows here experienced a transition from a freshwater lacustrine environment to a more brackish environment due to increasing influx of saline water from the Baltic Sea. The burrows reported are pyritic and show a range of crystal textures including framboidal, euhedral, microcrystalline masses and framboids with overgrowths of marcasite crystals. The framboidal texture indicates sufficient space for the crystals to grow so pyrite precipitation would occur in an open space (Thomsen and Vorren, 1984). Trace metal concentration was not the scope of this work but given the concentration of pyritic burrows within the sediments, lacustrine settings could sequester significant levels of trace metals.

4.2 Burrow enrichment relative to host sediment

The burrows discussed here all show an enrichment in trace elements relative to their host sediment as shown in Figure 2. Se mineralisation in Hock cliff burrows are 10 times richer than its host sediment, and Southerham burrows are around 4 times that of their host sediment. The burrows at Wren's nest did not show any Se mineralisation. Cu concentrations at both Wren's Nest and Hock Cliff burrows were 50 times greater than their host sediment, and Southerham burrows was 20 times that of its host sediment. Pb concentrations at both Wren's Nest and Southerham were 50 times greater than trace elements recorded in the host sediment. The Hock Cliff burrows were up to 100 times richer in Pb than its host sediment.

This shows that there is anomalous enrichment of trace elements in pyritic burrows relative to their hosts sediments. Trace element enrichment in burrows exceed the average values recorded for shale and carbonates and are comparable to values of the Gwna Group shales, which are regarded as protoliths to ore deposits.

4.3 Pyrite mineralisation

Burrows from Southerham and Hock cliff display framboidal textures, indicating that the pyrite had space to grow, and is also considered a signature of early stage microbial sulphate reduction (Fig. 6A

& B) (Schoonen, 2004; Virtasalo and Kotilainen, 2013). Early diagenetic framboidal pyrite in bioturbations have been shown to be richer in trace elements compared with pyrite not found in bioturbations (Lerouge et al., 2011). Southerham pyritic burrows show pyrite framboids with euhedral overgrowths (Fig. 6A). Euhedral pyrites are a secondary feature to the framboids and formed during diagenesis, recrystalising the original pyrite. Similar features are observed in SEM micrographs from Armstrong et al. (2018) and Virtasalo et al. (2010), which show framboidal pyrite with euhedral overgrowths.

The distribution of the metals within the burrows can give information about the timing of pyrite mineralisation. In the Hock Cliff burrows, as Pb and Se are concentrated in the burrow rim it is likely that they are from the same mineral phase. Lead selenide (clausthalite) is a common mineral phase found in pyrites. As Pb and Se are concentrated in the rim it suggests that it was enriched at a later stage, after early stage pyritization mediated by sulphate-reducing bacteria. Similar features are described by Parnell et al. (2017) and are attributed to hydrothermal Pb mineralisation during metamorphism. Fe and Cu are more evenly distributed throughout the burrow but are depleted at the burrow rim. This suggests that Cu was originally incorporated into the burrow at an early stage.

4.4 Oxidation of burrows and implication on metal concentration

The pyritic burrows reported here and elsewhere in the literature tend to be altered to Fe-oxide, as pyrite is commonly oxidized in the sedimentary environment (Rimstidt and Vaughan, 2003), giving the burrows a rusty colouration. Primarily this oxidation is only on surface exposures but in some cases, this weathering can penetrate to the core of the burrow. This has the potential to affect the distribution of trace metals, by remobilising trace metals which are soluble in oxidising conditions. Perez et al. (2019) demonstrated through LA-ICP-MS analysis of weathered pyrites that some trace elements were concentrated in a halo around the edge of the pyrite crystal, suggesting that certain trace elements are more persistent under oxidising conditions. Laser maps from Hock Cliff show that

Se & Pb are concentrated in a halo on the edge of the burrow and are depleted in the core of the burrow, which could be a result of preferential oxidation, redistributing Se within the burrow.

Regardless of the redistribution of metals, results shown here demonstrate that trace elements are preserved within burrows after oxidation, and therefore bioturbated sediments still represent a significant sink for trace metals, even after oxidative weathering.

4.5 Sequestration rates

Seafloor mining operations have focussed on deep marine Fe-Mn crusts as they are abundant in Se, Te and other trace elements. Although Fe-Mn crusts are rich sources of trace elements, they accumulate extremely slowly at 1-10 mm/Ma (Hein, 2000). Recent work by Armstrong et al. (2018) demonstrated that the black shales of the Gwna group have a Te sequestration rate greater than that of Fe-Mn crusts, highlighting the value of black shale for trace element sequestration.

The sequestration rates of Se, Pb & Cu were calculated using; the accumulation rates of each locality, which was calculated using the thickness and age of the unit they were sampled from; the measured density of each sample and the concentration of the element (in ppm) determined by LA-ICP-MS analysis. This information is summarised in table 1. Accumulation rates for each depositional environment were collated from existing literature and used to calculate sequestration ranges for the selected elements. This information is summarised in supplementary table 1.

Accumulation rates for a Cretaceous shallow shelf sea environment ranges from 6.4-100 m/Ma (Damholt and Surlyk, 2004; Friedman et al., 2016; Hopson, 2005; Kennedy and Garrison, 1975; Laurisden et al., 2009; Puckett, 1991; Surlyk and Lykke-andersen, 2007). Sequestration rates based on these accumulation rates and a measured density of 2.44 g/cm^3 are 900-13900 nmols/yr^{-1} for Se, 16300-253400 nmols/yr^{-1} for Cu and 24900-387400 nmols/yr^{-1} for Pb.

Accumulation rates for a Jurassic hemipelagic/pelagic environment ranges from 1.5-40 m/Ma (DeCelles and Currie, 1996; Hinnov and Park, 1999; Mattioli and Pittet, 2002; Simms et al., 2004). Sequestration rates based on these accumulation rates and a measured density of 2.72 g/cm^3 are 400-10600 nmols/yr^{-1} for Se, 31100-368100 nmols/yr^{-1} for Cu, and 6300-156000 nmols/yr^{-1} for Pb.

Accumulation rates for a Silurian carbonate platform environment ranges from 5.8-79 m/Ma (Bosscher and Schlager, 1993; Calner and Jeppsson, 2003; Cocks, 2004; Narbonne and Dixon, 1984; Soja, 1993). Sequestration rates based on these accumulation rates and a measured density of 2.87 g/cm^3 are 55000-745200 nmols/yr^{-1} for Cu and 15900-215500 nmols/yr^{-1} for Pb.

The sequestration rates of Se, Cu & Pb in Fe-Mn crusts are 0.5, 200 & 100, respectively. Conservative estimates of sequestration rates for all three depositional environments exceed those of Fe-Mn crusts. On average pyritic burrows sequester Se up to three orders of magnitude faster than Fe-Mn crusts. Cu and Pb are sequestered in pyritic burrows at two orders of magnitude greater than Fe-Mn crusts. Pb sequestration rates in pyritic burrows is the only element discussed here that is comparable to sequestration rates of Gwna Group sediments. Se and Cu burrow sequestration rates are two orders of magnitude lower than that of the Gwna Group. This shows that bioturbation can sequester metals more efficiently than Fe-Mn crusts, and bioturbated marine sediments could be regarded as a significant sink for trace elements.

5 Conclusion

The trace element data shows that bioturbated marine sediments have anomalous levels of trace elements preserved in pyritized burrows. The act of burrowing increases organic material in the sediment which drives bacterial sulphate reduction and the sequestration of trace elements. Specifically:

(i) When an organic rich reservoir is not available, trace elements can be concentrated into burrows which are rich in OM, which promotes pyritization and metal sequestration.

Bioturbated sediments across a range of geological ages show anomalous levels of trace elements preserved in pyritized burrows.

(ii) The three localities discussed here show an enrichment of Cu, Se, and Pb relative to their host sediments, despite oxidation which might weather and degrade the burrow.

(iii) Bioturbated sediments from Hock cliff, Wren's Nest and Southerham Grey Pit are more efficient at sequestering metals when compared with other deposits such as Fe-Mn crusts, which are regarded as rich sources of metals, but accumulate very slowly. Pyritic burrows can sequester Se up to three orders of magnitude faster than Fe-Mn crusts, and Pb and Cu up to two orders of magnitude faster than Fe-Mn crusts.

Acknowledgments

This work was supported by NERC grant NE/M010953/1. Electron Microscopy was performed with the help of J. Still in the ACEMAC Facility at the University of Aberdeen.

References

Antler, G., Mills, J. V, Hutchings, A.M., Redeker, K.R., Turchyn, A. V, 2019. The Sedimentary Carbon-Sulfur-Iron Interplay – A Lesson From East Anglian Salt Marsh Sediments. Front. Earth Sci. 7, 1–13. https://doi.org/10.3389/feart.2019.00140

Armstrong, J.G.T., Parnell, J., Bullock, L.A., Perez, M., Boyce, A.J., Feldmann, J., 2018. Tellurium, selenium and cobalt enrichment in Neoproterozoic black shales, Gwna Group, UK: Deep marine trace element enrichment during the Second Great Oxygenation Event. Terra Nov. 30, 244–253. https://doi.org/10.1111/ter.12331

Ayoola, P.B., Olayiwola, A.O., 2014. Trace Elements and major minerals evaluation of earthworm casts from a selected site in Southwestern Nigeria. ARPN J. Agric. Biol. Sci. 9, 216–218.

Berner, R.A., 1984. Sedimentary pyrite formation : An update. Geochim. Cosmochim. Acta 48, 605–

615.

Bosscher, H., Schlager, W., 1993. Accumulation Rates of Carbonate Platforms. J. Geol. 101, 345–355.

Bromley, R.G., 1996. Trace fossils: biology, taphonomy and applications (2nd ed), 361 pp. Chapman & Hall, London.

Buatois, L.A., Mángano, M.G., Minter, N.J., Zhou, K., Wisshak, M., Wilson, M.A., Olea, R.A., 2020. Quantifying ecospace utilization and ecosystem engineering during the early Phanerozoic—The role of bioturbation and bioerosion. Sci. Adv. 6, 1–12. https://doi.org/10.1126/sciadv.abb0618

Calner, M., Jeppsson, L., 2003. Carbonate platform evolution and conodont stratigraphy during the middle Silurian Mulde Event, Gotland, Sweden. Geol. Mag. 140, 173–203. https://doi.org/10.1017/S0016756802007070

Cocks, L.R.M., 2004. Palaeozoic: Silurian, in: Selley, R.C., Cocks, L.R.M., Plimer, I.R. (Eds.), Encyclopedia of Geology. Elsevier, Oxford, pp. 184–193. https://doi.org/10.1016/B0-12-369396-9/00047-2

Damholt, T., Surlyk, F., 2004. Laminated – bioturbated cycles in Maastrichtian chalk of the North Sea : oxygenation fluctuations within the Milankovitch frequency band. Sedimentology 51, 1323–1342. https://doi.org/10.1111/j.1365-3091.2004.00672.x

DeCelles, P.G., Currie, B.S., 1996. Long-term sediment accumulation in the Middle Jurassic – early Eocene Cordilleran retroarc foreland-basin system. Geology 24, 591–594.

Friedman, M., Beckett, H.T., Close, R.A., Johanson, Z., 2016. The english chalk and London Clay: Two remarkable British bony fish lagerstätten. Geol. Soc. Spec. Publ. 430, 165–200. https://doi.org/10.1144/SP430.18

Frimmel, H.E., 2009. Trace element distribution in Neoproterozoic carbonates as palaeoenvironmental

300 indicator. Chem. Geol. 258, 338–353. https://doi.org/10.1016/j.chemgeo.2008.10.033

301 Gingras, M.K., Pemberton, S.G., Smith, M., 2015. Bioturbation : Reworking Sediments for Better or
302 Worse. Oilf. Rev. 26(4), 46–58.

303 Harazim, D., McIlroy, D., Edwards, N.P., Wogelius, R.A., Manning, P.L., Poduska, K.M., Layne, G.D.,
304 Sokaras, D., Alonso-Mori, R., Bergmann, U., 2015. Bioturbating animals control the mobility of
305 redox-sensitive trace elements in organic-rich mudstone. Geology 43, 1007–1010.
306 https://doi.org/10.1130/G37025.1

307 Harazim, D., Virtasalo, J.J., Denommee, K.C., Thiemeyer, N., Lahaye, Y., Whitehouse, M.J., 2020.
308 Exceptional sulfur and iron isotope enrichment in millimetre-sized, early Palaeozoic animal
309 burrows. Sci. Rep. 10, 1–13. https://doi.org/10.1038/s41598-020-76296-8

310 Hein, J.R., 2000. Cobalt-rich ferromanganese crusts in the Pacific, in: Cronan, D.S. (Ed.), Handbook of
311 Marine Mineral Deposits. Boca Raton: CRC Press, pp. 239–279.

312 Hein, J.R., Koschinsky, A., Halliday, A.N., 2003. Global occurrence of tellurium-rich ferromanganese
313 crusts and a model for the enrichment of tellurium. Geochim. Cosmochim. Acta 67, 1117–1127.
314 https://doi.org/10.1016/S0016-7037(00)01279-6

315 Hein, J.R., Mizell, K., Koschinsky, A., Conrad, T.A., 2013. Deep-ocean mineral deposits as a source of
316 critical metals for high- and green-technology applications: Comparison with land-based
317 resources. Ore Geol. Rev. 51, 1–14. https://doi.org/10.1016/j.oregeorev.2012.12.001

318 Hein, J.R., Yeh, H.-W., Gunn, S.H., William, S. V, Benninger, L.M., Wang, C.-H., 1993. Two major
319 Cenozoic episodes of phosphogenesis recorded in equatorial Pacific seamount deposits.
320 Paleoceanography 8, 293–311.

321 Hinnov, L.A., Park, J.J., 1999. Strategies for assessing Early – Middle (Pliensbachian – Aalenian) Jurassic

cyclochronologies. Philos. Trans. R. Soc. Lodon 357, 1831–1859.

Hopson, P.M., 2005. A stratigraphical framework for the Upper Cretaceous Chalk of England and Scotland, with statements on the Chalk of Northern Ireland and the UK Offshore Sector. Br. Geol. Surv. Res. Rep. RR/05/01 102pp.

Hu, Z., Gao, S., 2008. Upper crustal abundances of trace elements: A revision and update. Chem. Geol. 253, 205–221. https://doi.org/10.1016/j.chemgeo.2008.05.010

Huerta-diaz, M.A., Tessier, A., Carignan, R., 1998. Geochemistry of trace metals associated with reduced sulfur in freshwater sediments. Appl. Geochemistry 13, 213–233.

Jean, G.E., Bancroft, G.M., 1986. Heavy metal adsorption by sulphide mineral surfaces. Geochim. Cosmochim. Acta 50, 1455–1463. https://doi.org/10.1016/0016-7037(86)90319-4

Jeans, C. V., Turchyn, A. V., Hu, X.-F., 2016. Sulfur isotope patterns of iron sulfide and barite nodules in the Upper Cretaceous Chalk of England and their regional significance in the origin of coloured chalks. Acta Geol. Pol. 66, 227–256. https://doi.org/10.1515/agp-2016-0010

Jensen, S., Droser, M.L., Gehling, J.G., 2006. A Critical Look at the Ediacaran Trace Fossil Record, in: Xiao, S., Kaufman, A.J. (Eds.), Neoproterozoic Geobiology and Paleobiology. Springer Netherlands, Dordrecht, pp. 115–157. https://doi.org/10.1007/1-4020-5202-2_5

Jørgensen, B.B., 1977. Bacterial sulfate reduction within reduced microniches of Oxidized Marine Sediments. Mar. Biol. 41, 7–17.

Kennedy, W.J., Garrison, R.E., 1975. Morphology and genesis of nodular chalks and hardgrounds in the Upper Cretaceous of southern England. Sedimentology 22, 311–386. https://doi.org/10.1111/j.1365-3091.1975.tb01637.x

343 Lalonde, S. V., Dafoe, L., Pemberton, S.G., Gingras, M.K., Konhauser, O, K., 2010. Investigating the
344 geochemical impact of burrowing animals: Proton and cadmium adsorption onto the mucus-
345 lining of Terebellid polychaete worms. Chem. Geol. 271, 44–51.

346 Large, R.R., Halpin, J.A., Danyushevsky, L. V, Maslennikov, V. V, Bull, S.W., Long, J.A., Gregory, D.D.,
347 Lounejeva, E., Lyons, T.W., Sack, P.J., Mcgoldrick, P.J., Calver, C.R., 2014. Trace element content
348 of sedimentary pyrite as a new proxy for deep-time ocean – atmosphere evolution. Earth Planet.
349 Sci. Lett. 389, 209–220. https://doi.org/10.1016/j.epsl.2013.12.020

350 Large, R.R., Halpin, J.A., Lounejeva, E., Danyushevsky, L. V, Maslennikov, V. V, Gregory, D., Sack, P.J.,
351 Haines, P.W., Long, J.A., Makoundi, C., Stepanov, A.S., 2015. Cycles of nutrient trace elements in
352 the Phanerozoic ocean. Gondwana Res. 28, 1282–1293.
353 https://doi.org/10.1016/j.gr.2015.06.004

354 Laurisden, B.W., Gale, A.S., Surlyk, F., 2009. Benthic macrofauna variations and community structure
355 in Cenomanian cyclic chalk – marl from Southerham Grey Pit , SE England. J. - Geol. Soc. 166,
356 115–127. https://doi.org/10.1144/0016-76492007-164.Benthic

357 Lerouge, C., Grangeon, S., Gaucher, E.C., Tournassat, C., Agrinier, P., Vinsot, A., Buschaert, S., 2011.
358 Mineralogical and isotopic record of biotic and abiotic diagenesis of the Callovian – Oxfordian
359 clayey formation of Bure (France). Geochim. Cosmochim. Acta 75, 2633–2663.
360 https://doi.org/10.1016/j.gca.2011.02.025

361 Mángano, M.G., Buatois, L.A., 2014. Decoupling of body-plan diversification and ecological structuring
362 during the Ediacaran-Cambrian transition: Evolutionary and geobiological feedbacks. Proc. R.
363 Soc. B Biol. Sci. 281. https://doi.org/10.1098/rspb.2014.0038

364 Mattioli, E., Pittet, B., 2002. Contribution of calcareous nannoplankton to carbonate deposition : a
365 new approach applied to the Lower Jurassic of central Italy. Mar. Micropaleontol. 45, 175–190.

366 Mitchell, R.H., 1968. A Semiquantitative Study of Trace Elements in Pyrite By Spark Source Mass
367 Spectrography. Nor. Geol. Tidsskr. 48, 65–80.

368 Narbonne, G.M., Dixon, O.A., 1984. Upper Silurian lithistid sponge reefs on Somerset Island, Arctic
369 Canada. Sedimentology 31, 25–50. https://doi.org/10.1111/j.1365-3091.1984.tb00721.x

370 Parnell, J., Brolly, C., Spinks, S., Bowden, S., 2016. Selenium enrichment in Carboniferous Shales, Britain
371 and Ireland: Problem or opportunity for shale gas extraction? Appl. Geochemistry 66.
372 https://doi.org/10.1016/j.apgeochem.2015.12.008

373 Parnell, J., Perez, M., Armstrong, J., Bullock, L., Feldmann, J., Boyce, A.J., 2017. A black shale protolith
374 for gold-tellurium mineralisation in the Dalradian Supergroup (Neoproterozoic) of Britain and
375 Ireland. Appl. Earth Sci. 126, 161–175. https://doi.org/10.1080/03717453.2017.1404682

376 Pemberton, S.G., Gingras, M.K., 2005. Classification and characterizations of biogenically enhanced
377 permeability. Am. Assoc. Pet. Geol. Bull. 89, 1493–1517. https://doi.org/10.1306/07050504121

378 Perez, M., Parnell, J., Armstrong, J., Bullock, L., Feldmann, J., 2019. Separation of selenium and
379 tellurium during low-temperature diagenesis, in: Mineral Resources for Green Growth, SGA. pp.
380 1808–1811.

381 Puckett, T.M., 1991. Absolute paleobathymetry of Upper Cretaceous chalks based on ostracodes -
382 Evidence from the Demopolis Chalk (Campanian and Maastrichtian) of the northern Gulf Coastal
383 Plain. Geology 19, 449–452.

384 Ray, D.C., Thomas, A.T., 2007. Carbonate depositional environments, sequence stratigraphy and
385 exceptional skeletal preservation in the Much Wenlock Limestone Formation (Silurian) of Dudley,
386 England. Palaeontology 50, 197–222. https://doi.org/10.1111/j.1475-4983.2006.00607.x

387 Rimstidt, D.D., Vaughan, D.J., 2003. Pyrite oxidation: A state-of-the-art assessment of the reaction

388 mechanism. Geochim. Cosmochim. Acta 67, 873–880. https://doi.org/10.1016/S0016-
389 7037(02)01165-1

390 Rudnick, R.L., Gao, S., 2003. Composition of the Continental Crust, in: Holland, H.D., Turekian, K.K.
391 (Eds.), Treatise on Geochemistry. Elsevier B.V., pp. 1–64.

392 Savrda, C.E., Daymond, P.A., Hespel, A.-M., 2016. Preservation of mucus trails by early pyritization in
393 Cretaceous Ingersoll shale (Eutaw Formation, eastern Alabama, U.S.A.). Palaios 31, 25–34.

394 Schieber, J., 2003. Simple Gifts and Buried Treasures—Implications of Finding Bioturbation and
395 Erosion Surfaces in Black Shales. Sediment. Rec. 1, 4–8. https://doi.org/10.2110/sedred.2003.2.4

396 Schoonen, M.A.A., 2004. Mechanisms of sedimentary pyrite formation, in: Geological Society of
397 America. pp. 117–134.

398 Seilacher, A., Palaios, S., Issue, T., Microbial, U., Feb, W., Seilacher, A., 1999. Biomat-Related Lifestyles
399 in the Precambrian. Soc. Sediment. Geol. 14, 86–93.

400 Shamberger, R.J., 1981. Selenium in the environment. Sci. Total Environ. 17, 59–74.
401 https://doi.org/10.1016/0048-9697(81)90108-X

402 Simms, M.J., Chidlaw, N., Morton, N., Page, K.N., 2004. British Lower Jurassic Stratigraphy, Geological
403 Conservation Review Series N 30. Peterborough: Joint Nature Conservation Committee.

404 Soja, C.M., 1993. Carbonate Platform Evolution in a Silurian Oceanic Island: A Case Study from Alaska's
405 Alexander Terrane. J. Sediment. Petrol. 63, 1078–1088.

406 Stüeken, E.E., Buick, R., Bekker, A., Catling, D., Foriel, J., Guy, B.M., Kah, L.C., Machel, H.G., Montañez,
407 I.P., Poulton, S.W., 2015. The evolution of the global selenium cycle: Secular trends in Se isotopes
408 and abundances. Geochim. Cosmochim. Acta 162, 109–125.

https://doi.org/10.1016/j.gca.2015.04.033

Sturdivant, S.K., Shimizu, M.S., 2017. In situ organism-sediment interactions: Bioturbation and biogeochemistry in a highly depositional estuary. PLoS One 12. https://doi.org/10.1371/journal.pone.0187800

Surlyk, F., Lykke-andersen, H., 2007. Contourite drifts, moats and channels in the Upper Cretaceous chalk of the Danish Basin. Sedimentology 54, 405–422. https://doi.org/10.1111/j.1365-3091.2006.00842.x

Sutherland, I.W., 2006. EPS-A complex mixture, in: Flemming, H.C., Wingender, J., Neu, T.R. (Eds.), The Perfect Slime-Microbial Extracellular Polymeric Substances. pp. 15–24.

Thomsen, E., Vorren, T.O., 1984. Pyritization of tubes and burrows from Late Pleistocene continental shelf sediments off North Norway. Sedimentology 31, 481–492. https://doi.org/10.1111/j.1365-3091.1984.tb01814.x

Virtasalo, J., Kotilainen, A., 2013. Iron isotope heterogeneity in pyrite fillings of Holocene worm burrows Iron isotope heterogeneity in pyrite fillings of Holocene worm burrows. Geology 41, 39–42. https://doi.org/10.1130/G33556.1

Virtasalo, J.J., Löwemark, L., Papunen, H., Kotilainen, A.T., Whitehouse, M.J., 2010. Pyritic and baritic burrows and microbial filaments in postglacial lacustrine clays in the northern Baltic Sea. J. Geol. Soc. London. 167, 1185–1198. https://doi.org/10.1144/0016-76492010-017

Weaver, P.P.., Schultheiss, P.J., 1983. Vertical open burrows in deep-sea sediments 2 m in length. J. Chem. Inf. Model. 301, 329–331.

Widerlund, A., Davison, W., 2007. Size and density distribution of sulfide-producing microniches in lake sediments. Environ. Sci. Technol. 41, 8044–8049. https://doi.org/10.1021/es071510x

Fig. 1 Map showing sampling localities of pyritic burrows. **a** – Wren's Nest, Nodular Beds Member, Silurian. **b** – Hock Cliff, Blue Lias Formation, Jurassic. **c** – Southerham Grey Pit, Zig Zag Chalk Formation, Cretaceous.

Table 1. Sequestration rates of bioturbated sediments. Average values used in this study and elsewhere; Fe-Mn crusts (Hein et al., 2013, 2003, 1993)**;** Gwna Group sediments (Armstrong et al., 2018); Wren's Nest formation age and thickness data (Cocks, 2004); Hock Cliff formation age and thickness data Simms et al. (2004); Southerham Grey Pit formation thickness and age data Hopson (2005). Average shale values taken from Hu and Gao (2008) and Stüeken et al. (2015). Hock Cliff and Wren's Nest burrow sample values obtained by LA-ICP-MS mapping. Host rock values for Hock Cliff & Wren's Nest were analysed for their bulk trace metal content by inductively coupled plasma-atomic emission spectrometry (ICP-AES) and inductively coupled plasma-mass spectrometry (ICP-MS), at ALS Laboratories, Loughrea, Ireland.

Fig. 2 Elemental content in parts per million (ppm) on the Y axis, sample localities on the X axis. Average shale values (Hu and Gao, 2008; Rudnick and Gao, 2003); Average carbonate values (Frimmel, 2009; Shamberger, 1981). Graphs are logarithmic as the average element values are considerably lower than found in pyritic burrows.

Fig. 3 LA-ICP-MS for Fe, Cu, Se and Pb in a pyritic burrow, Hock Cliff. Note the relative enrichments of Cu in the burrow centre, and Se and Pb in the outer burrow wall. Blue colours indicate lower trace element content, and red colours indicate higher trace element content.

Fig. 4 LA-ICP-MS for Fe, Cu, and Pb in a pyritic burrow, Wren's Nest. Note the relative enrichments of Cu & Pb are more evenly distributed throughout the burrow cross-section. Blue colours indicate lower trace element content, and red colours indicate higher trace element content.

Fig. 5 Summary diagram of pyritic burrow formation and metal enrichment in a marine sedimentary setting, adapted from (Virtasalo et al., 2010). Sulphate-reducing bacteria (SRB).

Fig. 6 A, Pyrite framboids with euhedral overgrowths, Southerham Grey Pit. B, Pyrite framboids, Hock Cliff. C, Euhedral and framboid pyrites weathered to iron oxides but still retain original pyritic morphologies, Southerham Grey Pit.

Highlights

- Trace elements (TE) are concentrated into burrows in marine sediments.
- Burrowing increases the amount of organic matter (OM) in the burrow.
- Increased OM drives bacterial sulphate reduction and metal sequestration.
- Bioturbated sediments show anomalous levels of TE preserved in pyritized burrows.
- Elements are sequestered at greater rates than in Fe-Mn crusts.

Figure 1

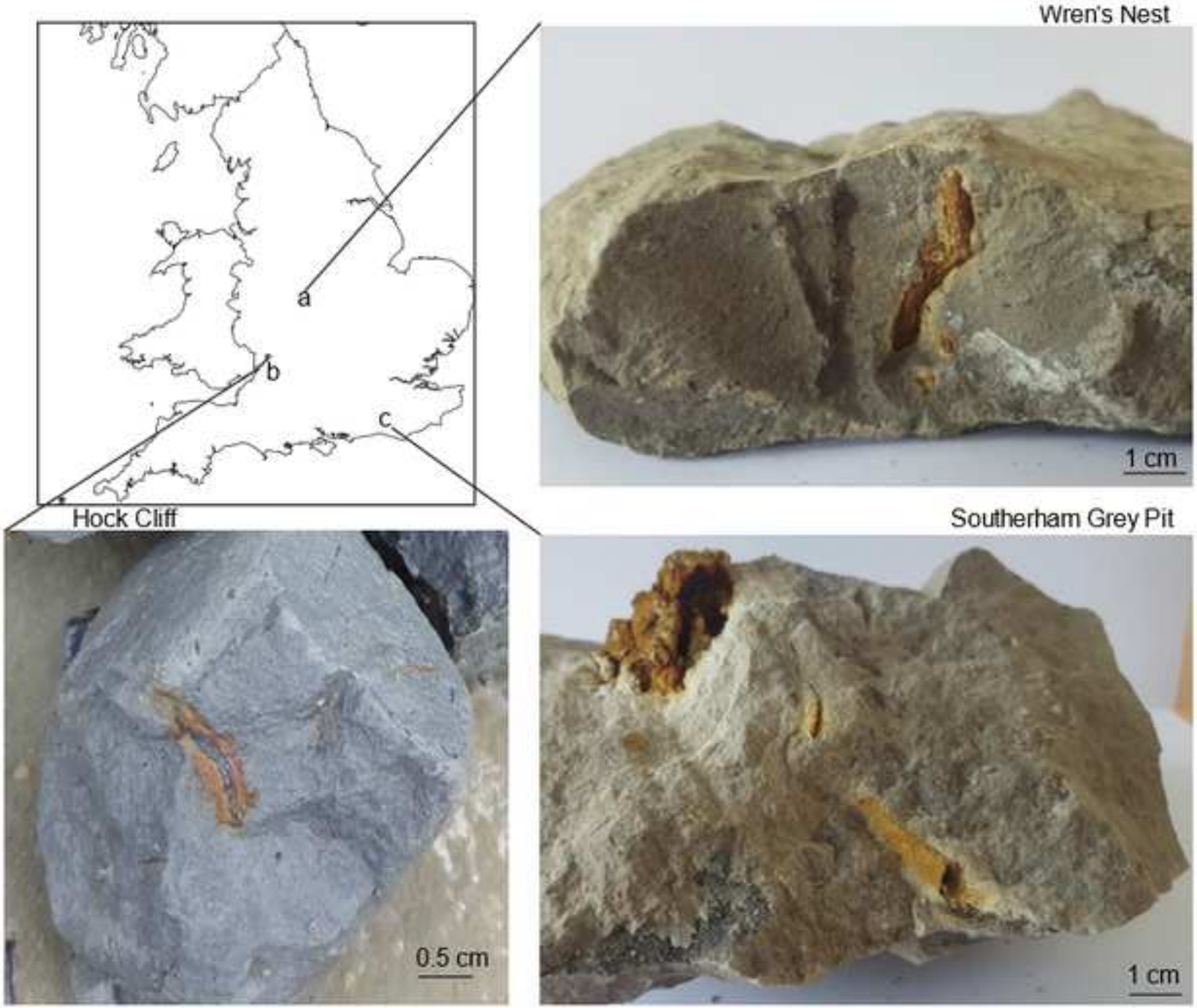

Figure 2

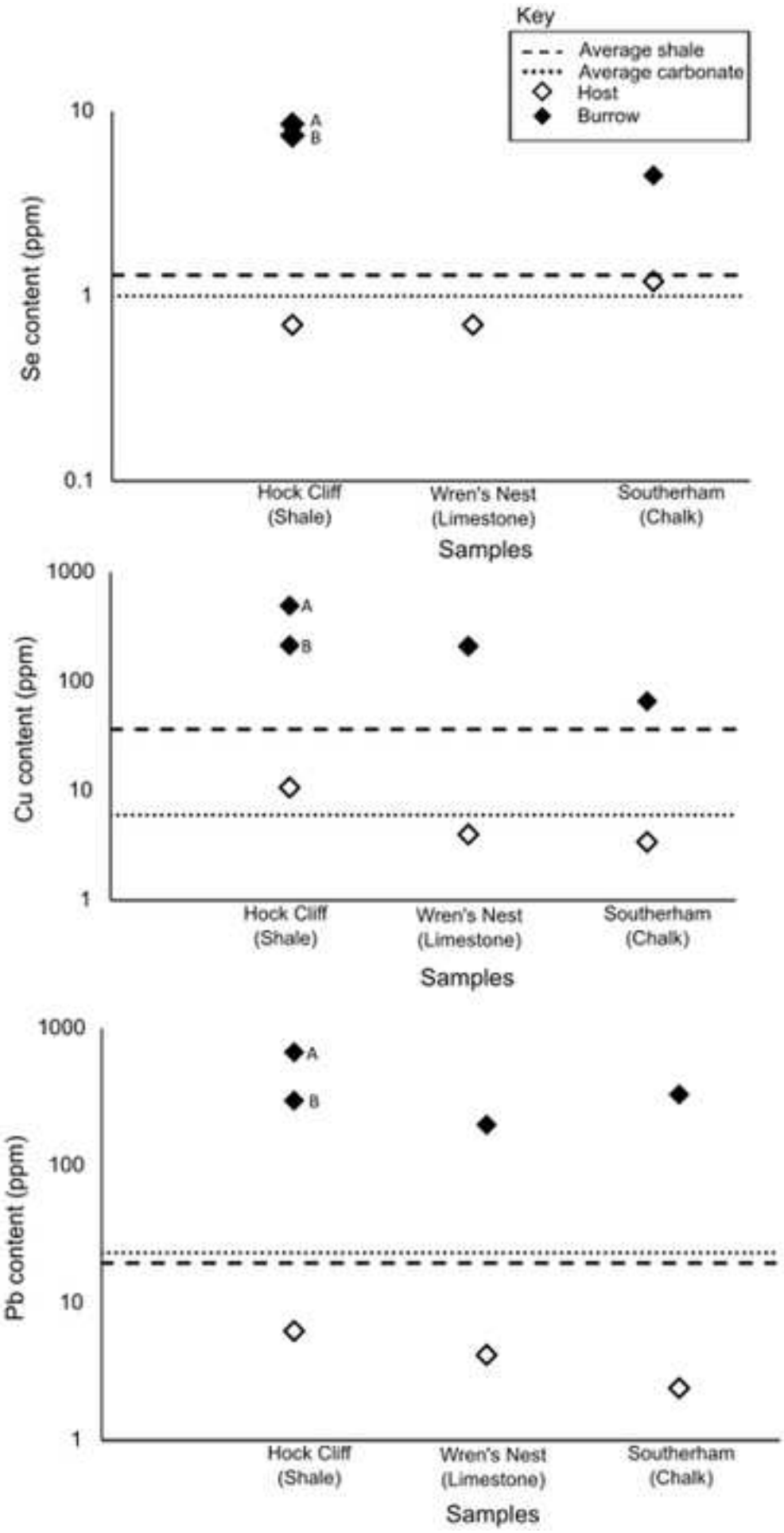

Figure 3

Click here to access/download;Figure;Brollyetal_Fig3.tif

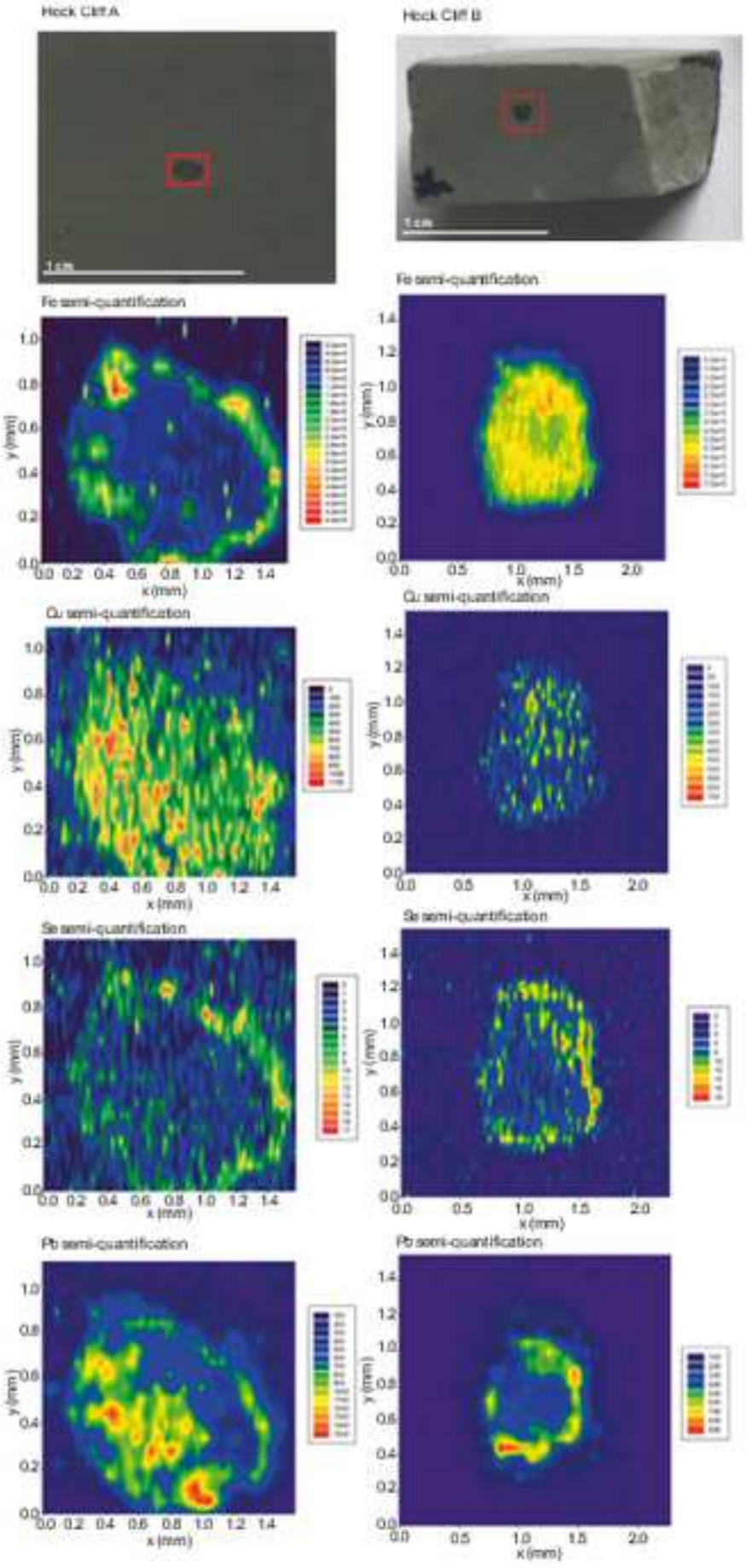

Figure 4

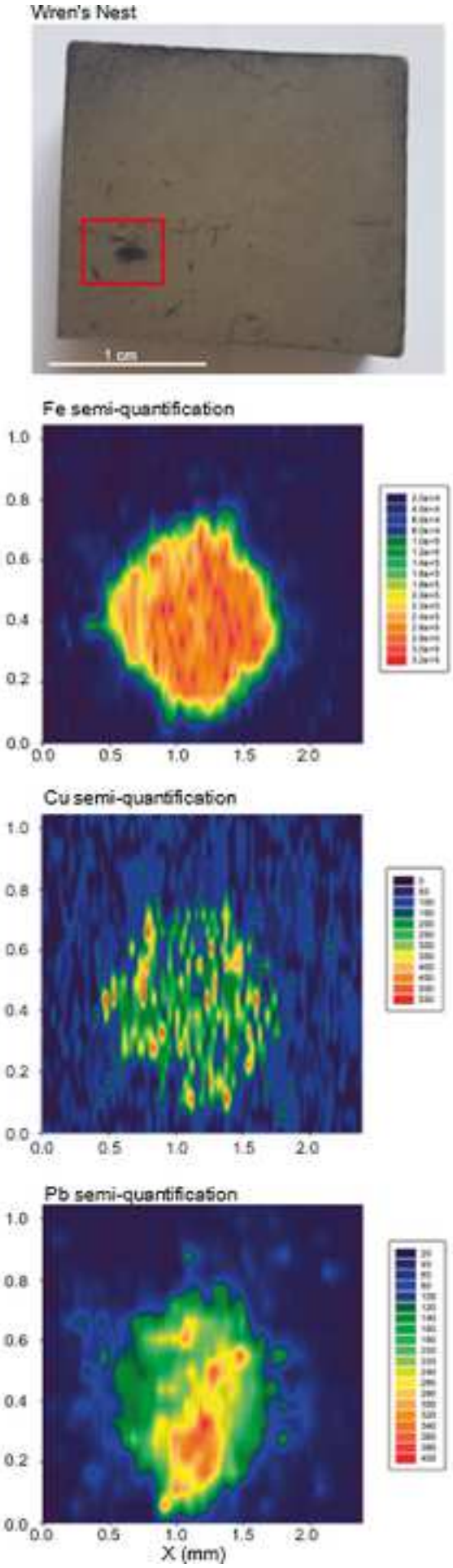

Figure 5

Click here to access/download;Figure;Brollyetal_Fig5.png

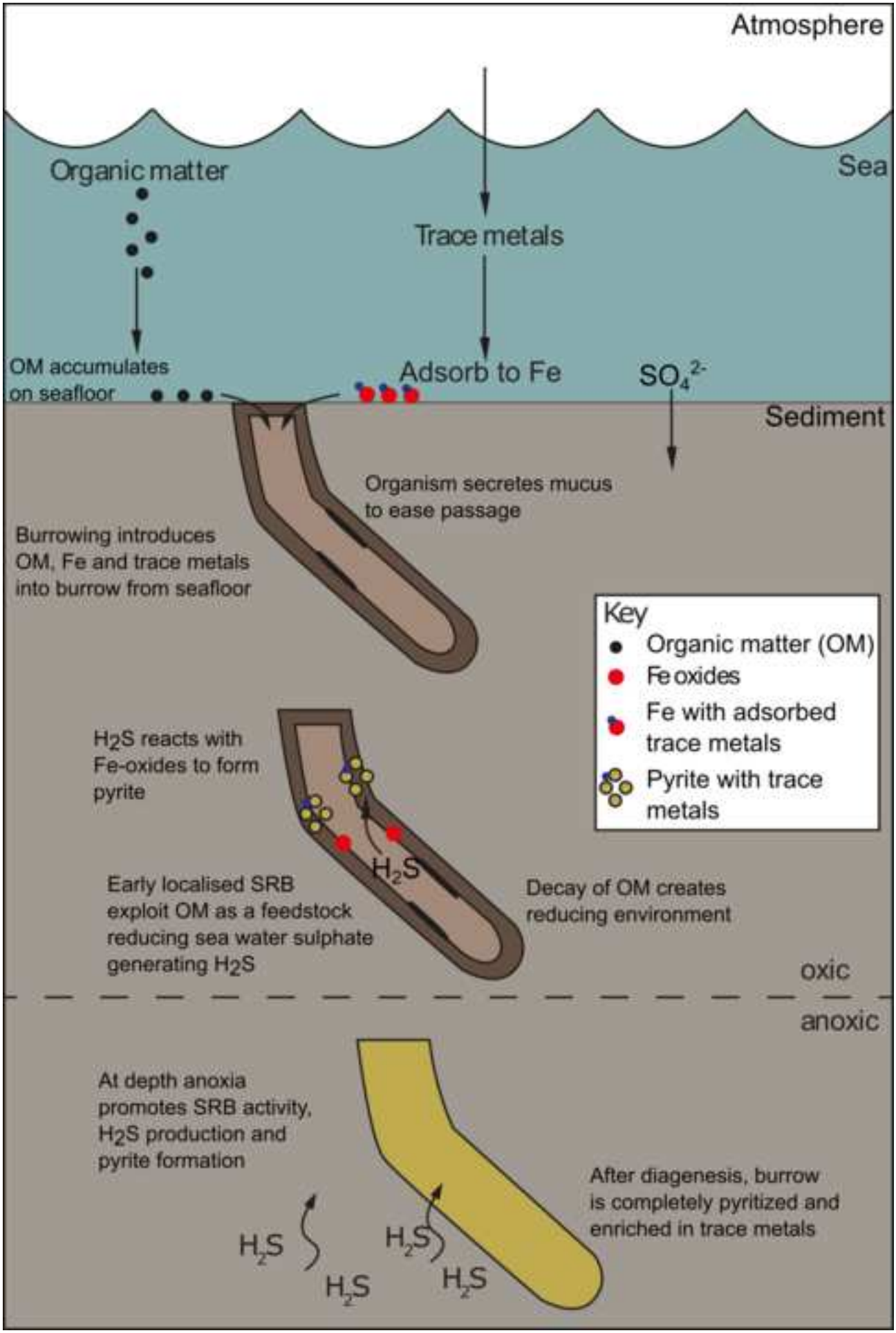

Figure 6

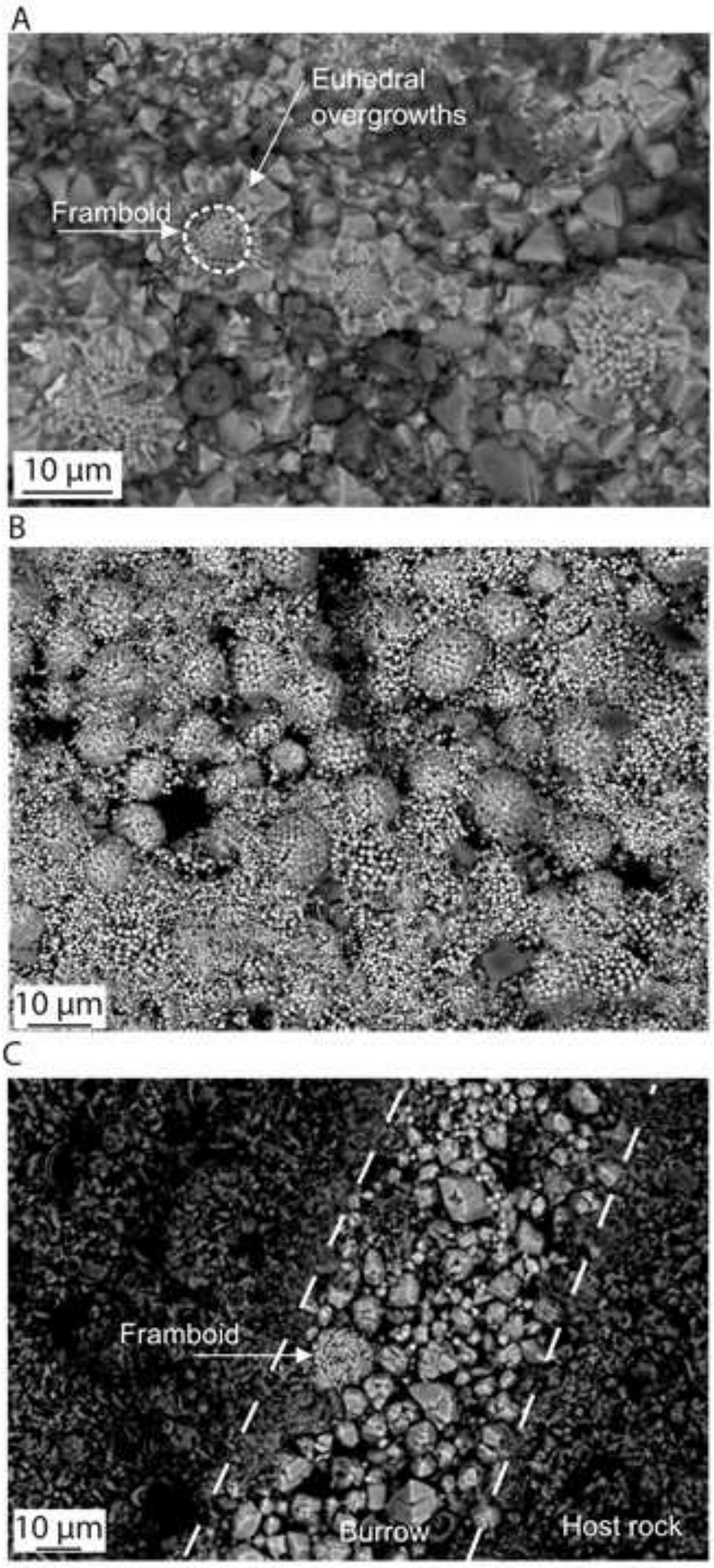

Table 1

Locality	Formation	Lithology	Environment	Amount of pyrite	Geological period	Age (Ma)	Thickness (m)	Density (g/cm3)	accumulation rate m/Ma	Se (ppm)	Cu (ppm)	Pb (ppm)	Se Sequestration rate (nmols/yr-1)	Cu Sequestration rate (nmols/yr-1)	Pb Sequestration rate (nmols/yr-1)
Wren's Nest	Much Wenlock Limestone Fm	Limestone	Shallow water/tropical carbonate platform	common	Silurian	429-424	29	2.87	5.8	-	210	198	-	55000	15900
Wren's Nest Host										0.7	4.0	4.2			
Hock Cliff A	The Blue Lias Fm	Rhythmic mudstones & limestones	Shallow - deeper water	abundant	Jurassic	201.3-190.8	17	2.72	1.6	8.2	494	669	500	34200	14200
Hock Cliff B										7.7	215	297	400	14900	6300
Hock Cliff Host										0.7	10.7	6.2			
Southerham Grey Pit	Zig Zag Chalk Fm	Chalk	Shallow shelf sea	abundant	Cretaceous	100.5-93.9	42.5	2.44	6.40	4.5	66	329	900	16300	24900
Southerham Grey Pit Host										1.2	3.4	2.4			
Fe-Mn Crusts					Eocene - present			1.3	0.1	3.2	926.9	1480.8	0.5	200	100
Gwna Group		Shale	Deep marine		Neoproterozoic	580-570		3.14	10	61.5	547.5	130.7	24500	270700	19900
Average Shale										1.3	36.5	19.5			
Average Carbonate										1	6	23.2			